AN $\mathcal{H}_\infty$ APPROACH TO CONTROL SYNTHESIS WITH LOAD MINIMIZATION FOR THE F/A-18 ACTIVE AEROELASTIC WING

Rick Lind[1]
NASA Dryden Flight Research Center

Abstract

The F/A-18 Active Aeroelastic Wing research aircraft will demonstrate technologies related to aeroservoelastic effects such as wing twist and load minimization. This program presents several challenges for control design that are often not considered for traditional aircraft. This paper presents a control design based on $\mathcal{H}_\infty$ synthesis that simultaneously considers the multiple objectives associated with handling qualities, actuator limitations, and loads. A point design is presented to demonstrate a controller and the resulting closed-loop properties.

Nomenclature

Acronyms

AAW	Active Aeroelastic Wing
SRA	Systems Research Aircraft

Symbols

A	actuator model for AAW
L	loads model for AAW
P	open-loop dynamics for AAW
T	closed-loop dynamics for SRA
K	controller
W	weighting function
δ	control surface position (*deg*)
$d\delta$	control surface rate (*deg/s*)
μ	structured singular value
$\mathcal{H}_\infty$	induced norm on transfer functions
Δ	uncertainty operator

Subscripts

ail	aileron
lei	leading-edge inboard flap
leo	leading-edge outboard flap
rud	rudder
tef	trailing-edge flap
stb	stabilator
in	input
out	output
701E	production F/A-18 controller

[1]Structural Dynamics, MS 4840/D, Edwards CA 93523, *rick.lind@dfrc.nasa.gov*

1. Introduction

The F/A-18 Active Aeroelastic Wing (AAW) research testbed is being developed to demonstrate aeroservoelastic technology [7]. The main concept of this technology is the active use of aeroelasticity to maneuver the aircraft. Many aspects of the technology have been initially studied in wind tunnel tests; however, the AAW aircraft is a full-scale system from which information for future designs can be derived [8].

One important aspect of the AAW program will be the use of wing twist to produce rolling moments. Controllers designed using rigidity assumptions move the ailerons to generate roll but the wing flexibility acts to oppose this roll. Roll reversal is defined at a dynamic pressure at which the flexibility actually causes a roll in the opposite direction than is desired [3]. Controllers for the AAW will generate roll by moving the leading-edge surfaces to create a wing twist and thus be able to efficiently operate past the roll reversal of the ailerons.

The issue of load minimization is also an important aspect of AAW technology that will be addressed by the flight program. Essentially, the wing should experience reduced loads because the control surfaces are not inducing a large load to overcome wing twist; rather, the surfaces promote wing twist in an efficient manner. The reduction in loads may allow a reduction in structural weight and consequently reduce production and operating costs of future aircraft.

This paper presents an approach to design a flight controller for the F/A-18 AAW aircraft using an $\mathcal{H}_\infty$-synthesis framework. This framework is particularly useful because several objectives and constraints can be directly included in the synthesis. The resulting controllers can be efficiently computed and an approximation can be realized that conforms to a desired architecture.

A closed-loop model of the AAW airplane is presented as a design example to demonstrate the design methodology and resulting properties. This example shows the $\mathcal{H}_\infty$ controller is able to constrain loads and achieve desired levels of handling qualities and roll performance without violating actuator limitations.

This paper provides a limited presentation of the actual $\mathcal{H}_\infty$ controller to be flown on the aircraft. Firstly, only the lateral-directional dynamics will be discussed because the roll performance is of more interest than the pitch performance. Secondly, a gain-scheduled controller has been formulated but only a point design is presented for brevity. Thus, the purpose of this paper is to present the general design methodology whereas future papers will present the final design and flight test results.

2. Closed-Loop Objectives

The fundamental objective of the AAW program is to investigate technologies related to the utilization of aeroservoelasticity for modeling and control of flexible aircraft. These technologies include open-loop concepts such as modeling and closed-loop concepts such as commanding wing twists and controlling loads. The controller for the aircraft must be designed to allow flight tests that can achieve the program objectives; however, these objectives are only indirectly considered for control synthesis. There are several related closed-loop objectives that are actually used to design controllers.

Several of the closed-loop objectives are essentially applicable to any aircraft and are required for flight safety. The most basic of these objectives is to stabilize the aircraft within a flight envelope. Another objective is to provide handling qualities that are at or near Level 1 ratings for a variety of maneuvers. Finally, the controller must avoid saturating actuator positions and rates except for minor and brief saturation that may be allowed in response to full-stick commands from the pilot.

Some of the controller objectives are specific to AAW technology. One of these objectives is to maximize the roll performance of the aircraft. Previous wind tunnel experiments have indicated that wing twist may provide large amounts of control authority so the AAW program seeks to demonstrate this on a full-scale vehicle [9].

Another objective is to reduce the maneuvering loads throughout the structure. This objective requires more of a formal definition than the others because it may not be immediately obvious how to select a preferred set of loads. For example, some controllers may reduce bending but increase torsion whereas others may reduce torsion by sacrificing bending. Similarly, the relative amount of loads at the wing root and fold must be considered when defining the concept of reduced loads.

An additional objective that is being enforced is that the controller must be realized with an acceptable architecture. This objective is not necessarily an AAW technology; however, it is important to facilitate the flight test. $\mathcal{H}_\infty$ synthesis generally generates high-order controllers

that are difficult to implement on a flight computer. Alternative controllers for the AAW have been proposed that use extensive scheduling over flight condition and also aircraft states such as roll rate and acceleration [11]. The $\mathcal{H}_\infty$ controller will be required to utilize a low-order filter with gain tables that are scheduled over standard flight condition variables.

Furthermore, all these objectives must be achieved without using the stabilator to generate roll moments. This constraint is important because the production aircraft uses the stabilator to generate almost the entire roll moment when flying at high dynamic pressures. Thus, the controller will have to compensate for the loss of this powerful control surface by commanding wing twist through the aeroservoelastic dynamics of the wing.

The flight test program for the AAW will be limited to a flight envelope that allows the technology to be efficiently demonstrated. This envelope has a subsonic region that covers Mach number from .85 to .95 and altitudes from 5 kft to 15 kft. A supersonic region is also included that covers Mach number from 1.1 to 1.3 and altitudes from 10 kft to 25 kft. A remaining objective is for the controller to operate at any flight condition within these regions.

3. Controller Architecture

The controller architecture for the $\mathcal{H}_\infty$ design is chosen to match that of the controller on the production F/A-18 aircraft. This standard controller is denoted as K_{701E} [5]. The architecture involves several first-order filters and a set of gains that are scheduled over Mach number and altitude. The filters are used for stick shaping, response determination, and notching of aeroelastic modes.

The formulation of the gains and filters may require an indirect computation because standard tools for $\mathcal{H}_\infty$ synthesis do not compute a structured controller [2]. The realization will be accomplished by synthesizing a full-order controller that minimizes the $\mathcal{H}_\infty$ norm of the closed-loop system and then employing an approximation to the dynamic compensator. Basically, the essential frequency-domain characteristics of the full-order controller will be captured and a first-order system that approximates these characteristics will be used for control.

The controller can be formulated in the $\mathcal{H}_\infty$ framework using only information about the open-loop plant but the design of the AAW controller can be simplified by taking advantage of elements from the K_{701E} controller. Specifically, directional control provided by the commands to the rudder is anticipated to be adequate for both the standard F/A-18 and the AAW airplane. Thus, K_{AAW} will generate gains for the wing surfaces from an $\mathcal{H}_\infty$ synthesis and use gains for the rudder from K_{701E}.

The measurements used to generate lateral control are stick command and roll rate. These measurements are chosen to match the signals that are used by K_{701E} to generate commands for the wing control surfaces so that K_{AAW} and K_{701E} have the same architecture and measurement paths. The outputs of the lateral controller are commands to the aileron, leading-edge inboard and outboard flaps, and trailing-edge flap.

The complete lateral-directional controller, K_{AAW}, is composed of the gain matrix, G, and first-order filter, $F(s)$, to generate commands for the wing control surfaces and also K_{701E} to generate commands for the rudder as shown in Figure 1. Note the stabilator command is generated by a 0-gain element to ensure the horizontal tails are not used for rolling maneuvers.
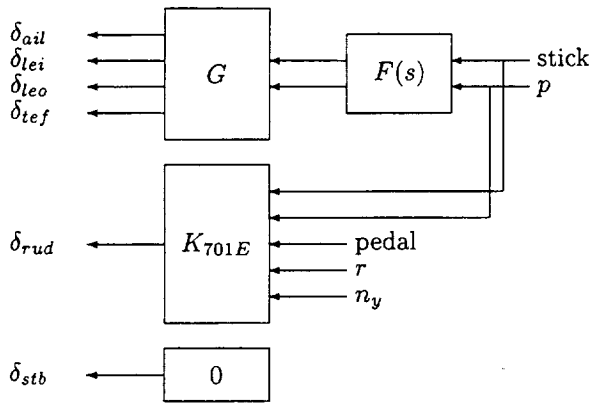

Figure 1: Architecture of K_{AAW}

4. Control Design Approach

The standard framework for $\mathcal{H}_\infty$ synthesis is to formulate a design model such that the objective is to minimize the $\mathcal{H}_\infty$ norm of the closed-loop system [4]. This objective is equivalent to minimizing the largest output that results from any bounded input signal. Thus, the design model must include a set of error signals that should be small if the closed-loop objectives are satisfied.

One of the error signals in the design model is used to ensure the AAW aircraft has acceptable handling qualities. This error signal can be generated by considering traditional metrics for linear models; however, the design for the AAW controller can be simplified by taking advantage of current F/A-18 controllers. Specifically, the Systems Research Aircraft (SRA) is an F/A-18 that operates with the K_{701E} controller and represents a model with acceptable handling qualities [10].

The error signal for handling qualities is defined by requiring the closed-loop response of the AAW airplane to be similar to the closed-loop response of the SRA airplane. This design approach is often called model fol-

lowing or model matching in reference to the objective of making the closed-loop characteristics of a model match the characteristics of another model [1]. The handling qualities of an aircraft are qualitative evaluations of response characteristics so matching the closed-loop AAW and SRA models should attempt to make their handling qualities similar also.

Define a linear system, T, to represent the closed-loop model of the SRA with K_{701E}. The inputs to this model are pilot commands through the lateral stick and rudder pedal and the outputs are the measured values of roll rate, yaw rate, and lateral acceleration. An error signal, e_P, is defined by weighting the subtracted output of T and the corresponding measurements of the AAW.

The weighting function associated with e_P is used to indicate the acceptable levels of difference between the AAW and SRA responses. Essentially, this weighting is the inverse of the acceptable differences such that if $\|e_P\|$ is less than 1 then the error is acceptable. The weighting is frequency-varying to reflect a desire for good tracking performance at low frequencies but allow larger errors at high frequencies.

Define W_P as the performance weighting associated with the model-following error of e_P. The diagonal elements of this weighting are the filters associated with errors in roll rate, yaw rate, and lateral acceleration. For example, the difference in roll rate for the low-frequency response of the AAW and SRA models is desired to be less than 1.15 deg/s so the weighting function has $\frac{1}{1.15} = .87$ as the low-frequency magnitude. Also, the bandwidth of the filter is chosen by placing a pole at .1 rad/s to denote the frequency range over which performance is desired. Similar elements of W_P are using a 3.5 weight for yaw rate error and .02 weight for lateral acceleration error.

$$W_P = \begin{bmatrix} \frac{.87}{1000}\frac{s+100}{s+.1} & 0 & 0 \\ 0 & \frac{3.5}{1000}\frac{s+100}{s+.1} & 0 \\ 0 & 0 & \frac{.02}{1000}\frac{s+100}{s+1} \end{bmatrix}$$

The desire to track only low-frequency responses is also reflected by filtering the stick command. This filter, W_u, is chosen with a maximum magnitude of 3 to reflect that the largest stick command is 3 in. Also, the bandwidth of the filter is chosen to reflect the types of stick motions that are often encountered during maneuvering.

$$W_u = .03\frac{s+5000}{s+50}$$

Another error signal, e_K, is defined to penalize actuator commands such that a large error implies a large actuator command. Associated with this error is a penalty filter to indicate the acceptable magnitudes and rates of the actuator commands. The low-frequency magnitude of this penalty is chosen as the inverse of the position limit of the actuator and the high-frequency magnitude

is chosen to be large to penalize any high-frequency commands. Also, the bandwidth of this filter is chosen to match the actuator bandwidth and ensure the controller does not cause rate saturation.

Define W_K as the weighting associated with the actuator penalty. The filters along the diagonal note frequency-varying upper bounds on the allowable commands to the control surfaces. For example, the leading-edge outboard flaps are limited to positions with magnitudes less than 15 *deg* so the low-frequency magnitude of the penalty weighting on δ_{leo} and δ_{lei} is .066 as determined by the inverse of the allowable magnitude. The zero of the filter at 4 *rad/s* is chosen to shape the response near the actuator bandwidth of approximately 0.7 *rad/s*. Similar elements of W_K are chosen to penalize the other actuators with .02 low-frequency weight on ailerons and .038 low-frequency weight on trailing-edge flaps.

$$W_K = \begin{bmatrix} 2.0\frac{s+40}{s+4000} & 0 & 0 & 0 \\ 0 & 6.6\frac{s+4}{s+400} & 0 & 0 \\ 0 & 0 & 6.6\frac{s+4}{s+400} & 0 \\ 0 & 0 & 0 & 3.8\frac{s+40}{s+4000} \end{bmatrix}$$

The design model must also include an error signal that represents the objective of load reduction. The approach does not explicitly perform a load minimization; rather, desired loads are noted such that the synthesis computes a controller that restricts the induced loads to be less than these desired loads during a closed-loop maneuver.

The desired loads are chosen based on analysis of the approximate loads encountered by the SRA in response to pilot commands. The bending moments at the wing root and fold are chosen to be similar in magnitude to the SRA responses. The torsion moments at the wing root and fold are allowed to be 4-times greater for the AAW than for the SRA airplane to allow for wing twist. Various values of desired loads were considered but the chosen loads lead to a controller that is able to satisfy the load objective while also satisfying handling qualities and actuator objectives.

An error signal, e_L, is defined as the weighted loads of the AAW. The weighting, W_L, is used to indicate the acceptable levels of loads and penalize loads that are above the desired levels. This error and weighting affect the moments for root bending, root torsion, fold bending, and fold torsion of the wing. A similar error, e_M, is defined by considering the hinge moments on the AAW control surfaces. This error is defined as the weighted values of the hinge moments for the aileron, leading-edge inboard flap, leading-edge outboard flap, and trailing-edge flap of the wing. The rudder could also be included in this error but it does not encounter large moments so it was omitted to reduce complexity of the design model. A weighting, W_M, is used to indicate the maximum moments that can be encountered and ensure that if $\|e_M\|$

is less than 1 then the hinge moments do not violate any structural constraints

$$W_L = \frac{s+1000}{s+.001} * $$

$$\begin{bmatrix} 50.0\frac{s+.03}{s+10} & 0 & 0 & 0 \\ 0 & 6.0\frac{s+.03}{s+10} & 0 & 0 \\ 0 & 0 & 30.0\frac{s+.01}{s+10} & 0 \\ 0 & 0 & 0 & 1.5\frac{s+.01}{s+10} \end{bmatrix}$$

$$W_M = \begin{bmatrix} \frac{1}{48000} & 0 & 0 & 0 \\ 0 & \frac{1}{333000} & 0 & 0 \\ 0 & 0 & \frac{1}{80000} & 0 \\ 0 & 0 & 0 & \frac{1}{130000} \end{bmatrix}$$

The design model used for controller synthesis that includes the error signals is shown in Figure 2. This model denotes P as the open-loop dynamics model of the AAW and L as the loads model of the AAW vehicle.
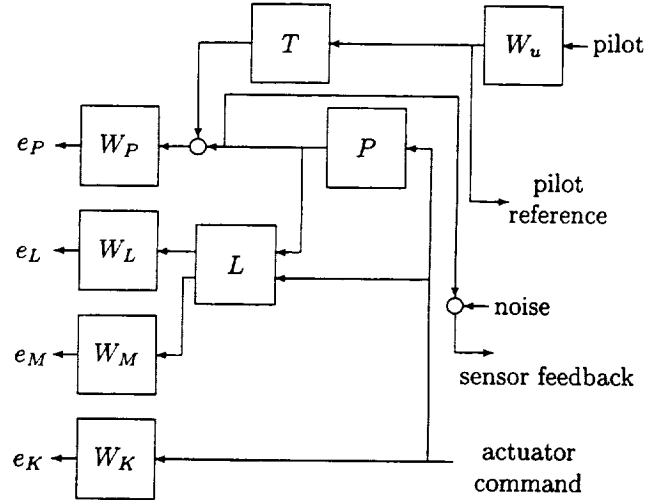

Figure 2: Synthesis Model for Control Design

The resulting controller, K_{AAW}, is actually a structured system that contains elements of K_{701E} as shown in Figure 1. Thus, the synthesis is actually intended to compute only the first-order filter and a set of gains; however, standard algorithms compute an unstructured state-space controller [2]. The procedure to be used for control design is to initially compute a state-space controller that relates the stick command and roll rate measurement to the commands for the wing control surfaces. This initial controller will then be approximated as a first-order filter and a set of gains by analyzing the Bode plot of the dynamical realization. The closed-loop properties are not guaranteed to be similar for the vehicle with the dynamic controller and the approximation; however, the design example demonstrates that such an approximation can be formulated for this aircraft without severely degrading the closed-loop responses.

26

5. Point Design

5.1. Controller Synthesis

A point design of a controller is computed for the model that represents the AAW in the center of the supersonic envelope at Mach number 1.2 and an altitude of 15 *kft*. This model was chosen because it is considered to be representative of the general dynamics of the models throughout the supersonic regime.

The controller is computed to minimize the $\mathcal{H}_\infty$ norm of the closed-loop design model. The resulting norm is 1.12 and is slightly greater than the desired norm of 1; however, the objectives are violated by at most 12 percent so this controller achieves reasonable performance levels for the design model.

The objectives that are driving the control design are trying to achieve good handling qualities while avoiding actuator saturation. In particular, the closed-loop $\mathcal{H}_\infty$ norm reflects properties of the transfer function from the stick to the performance objective for roll rate and from the stick to the actuator constraint on the leading-edge inboard flap. This implies the control synthesis is inherently limited by balancing the tradeoff between handling qualities and actuator constraints. Thus, attempting to minimize the loads, rather than simply reducing the loads, will cause a further tradeoff and result in larger violations of either the handling qualities or actuator objectives.

The initial realization of the controller is a state-space system with 60 states. Model reduction algorithms can reduce this dimension to 10 states without causing a noticeable degradation in performance; however, the desired architecture requires a first-order filter and gain implementation. An approximation of the controller that allows this implementation can be realized by considering the Bode plots of the transfer function from stick to the leading-edge surface commands as shown in Figure 3.

A notable feature of these frequency responses is their similarity to frequency responses of first-order filters. In particular, the magnitude and phase show little variation with frequency until 10 *rad/s* and then the magnitude shows a first-order rolloff. This behavior suggests a controller realization of a first-order filter that has a pole at 10 *rad/s* and a magnitude that matches the low-frequency magnitude of Figure 3.

A similar approximation must be performed to generate the gains that produce trailing-edge surface commands from controller inputs. The Bode plots of the corresponding transfer functions of the dynamic controller are shown in Figure 4. These plots show that a first-order approximation can not accurately capture the dynamics of the full-order controller; however, the approximation can still loosely represent the general features.
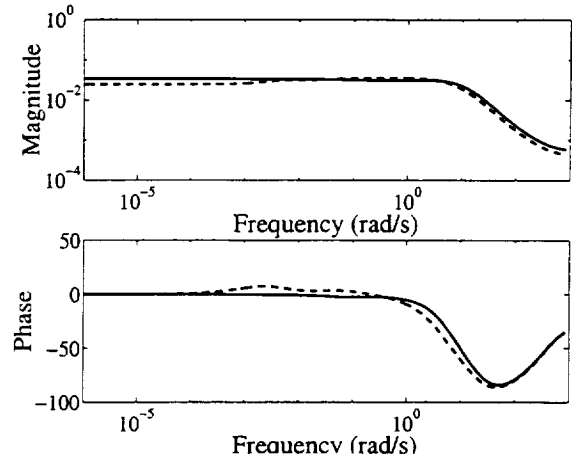
Figure 3: Bode Plot of the Dynamic Controller from Stick to Control Surface Command for Leading-Edge Inboard Flap (—) and Outboard Flap (— — —)
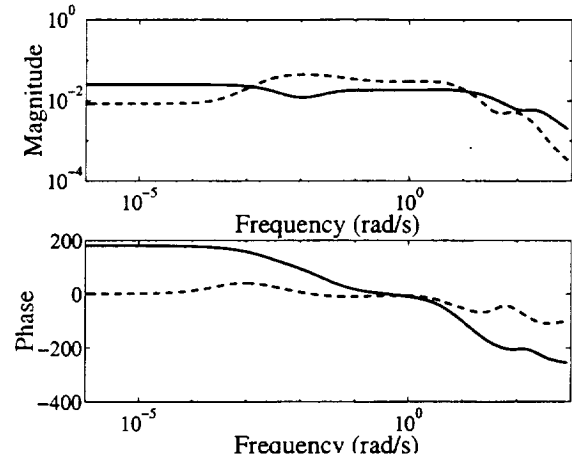
Figure 4: Bode Plot of the Dynamic Controller from Stick to Control Surface Command for Aileron (—) and Trailing-Edge Flap (— — —)

The approximation procedure is applied to the entire controller for both stick and roll rate inputs using the same first-order filter. The only parameters that are allowed to vary are the magnitude of the gains for each channel. This type of approximation is necessary because the implementation requires a single filter to be used. The resulting elements of K_{AAW}, labeled G and $F(s)$ in Figure 1, can be realized as a filter and matrix combination.

$$
\begin{bmatrix} \delta_{ail} \\ \delta_{lei} \\ \delta_{leo} \\ \delta_{tef} \end{bmatrix} = .01 \frac{s + 1000}{s + 10} \begin{bmatrix} -0.025 & -7.0 \times 10^{-6} \\ 0.034 & -5.0 \times 10^{-7} \\ 0.025 & -1.1 \times 10^{-6} \\ 0.008 & -1.2 \times 10^{-5} \end{bmatrix} \begin{bmatrix} \text{stick} \\ p \end{bmatrix}
$$

K_{AAW} has several features that can be related to K_{701E}. Firstly, the gains in different columns of the matrix have predominately different signs. This indicates the surface

commands are actually generated by a weighted difference between stick command and measured roll rate in a similar fashion as K_{701E}. The aileron command appears to differ from this structure but actually this flight condition is beyond roll reversal so the aileron has the opposite behavior of the leading-edge surfaces.

Another feature is the magnitude difference between the gains for the stick command and roll rate feedbacks. This difference matches the behavior of K_{701E} and weights the stick command larger than the roll rate. Essentially, the lateral-directional controller is like an open-loop gain that does not strongly depend on feedbacks.

The closed-loop model of the AAW with K_{AAW} is not guaranteed to have similar properties as the closed-loop model of the AAW with the full-order dynamic controller; however, the controller approximation is not anticipated to dramatically degrade closed-loop performance. Consider that the leading-edge surfaces are the main effectors for roll performance and handling qualities. The controller elements that generate commands for these surfaces are quite similar between the dynamic controller and K_{AAW} so the performance should be similar. Conversely, the commands for the trailing-edge surfaces are not generated by a high quality approximation but these commands do not strongly affect roll performance. Thus, the approximation used to formulate K_{AAW} should not drastically alter the closed-loop properties as compared to the full-order $\mathcal{H}_\infty$ controller.

5.2. Linear Simulation

Time responses of the closed-loop system are simulated using a linear model of the lateral-directional dynamics and K_{AAW}. These simulations do not include all aspects of the aircraft and so are not intended to accurately predict the responses of the full-order nonlinear system. Despite this limitation, the simulated responses are valuable to consider because they demonstrate if the methodology is able to compute a controller that achieves the desired closed-loop objectives for a general model.

One of the main performance objectives of the control design is to match handling qualities for the AAW and SRA. There are several criteria used to evaluate handling qualities but a simple way to roughly compare handling qualities is to compare transient responses. Essentially, if the aircraft respond similarly then their handling qualities, which are based on response characteristics, are probably also similar. Responses from the AAW with K_{AAW} and the SRA with K_{701E} are simulated in response to a doublet command through the lateral stick as shown in Figure 5.

This stick command is chosen to demonstrate several closed-loop properties. The initial command of 1.5 *in* is a half-stick command so the AAW response and han-
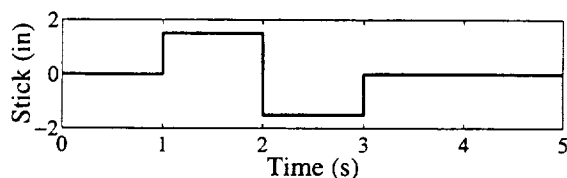
Figure 5: Stick Command

dling qualities should closely match the SRA performance without saturating the actuators. The response to this command should demonstrate half of the maximum roll rate that can be achieved with K_{AAW}. The second command of 3 *in* will demonstrate the full-stick response and indicate if excessive saturation is commanded.

The responses of the body-axis orientation angles to the lateral stick command are shown in Figure 6. The similarity of the AAW and SRA responses demonstrates the controller is able to achieve the desired model-following, and consequently handling qualities, characteristics.
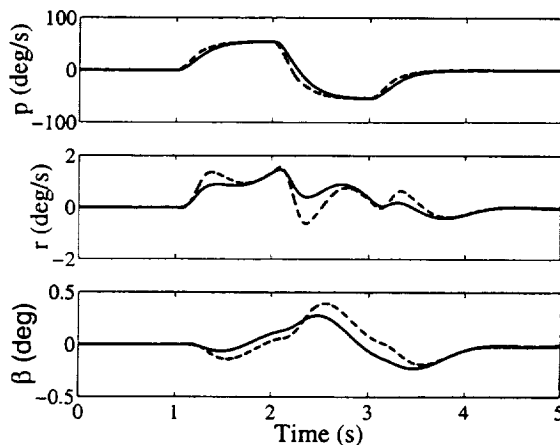
Figure 6: Sensor Measurements during Doublet Maneuver : AAW (—), SRA (– – –)

There are several features in the roll rate responses of Figure 6 that can be used to evaluate the performance of K_{AAW}. One feature is the similarity in roll rate that is achieved for the half-stick command. Both aircraft show roll rates near 55 deg/s so the maximum roll rate for the AAW is 110 *deg/s* in response to a full-stick command. This roll rate satisfies the performance objective of matching the maximum roll rate for the AAW and SRA. There is a slight lag in the AAW response as compared to the SRA; however, the small delay should not overly affect handling qualities and can perhaps be altered by simply tweaking the controller gains.

The remaining responses of Figure 6 also demonstrate interesting features. The angle of sideslip in the responses is similar in both magnitude and direction and this is an important factor in determining handling qualities.

28

Also, the yaw rate shows some difference between AAW and SRA responses so the elements of K_{701E} that are used in K_{AAW} may have to be slightly altered because K_{701E} does not account for the altered roll dynamics.

Figure 7 presents the control surface positions for each aircraft in response to the stick doublet. These positions demonstrate the actuator positions are not saturated during the transient maneuver despite the stick being moved to half of its maximum position. These linear results demonstrate that the leading-edge inboard flap would be slightly position saturated for a full 3 *in* stick command; however, the remaining surfaces would not be position saturated.
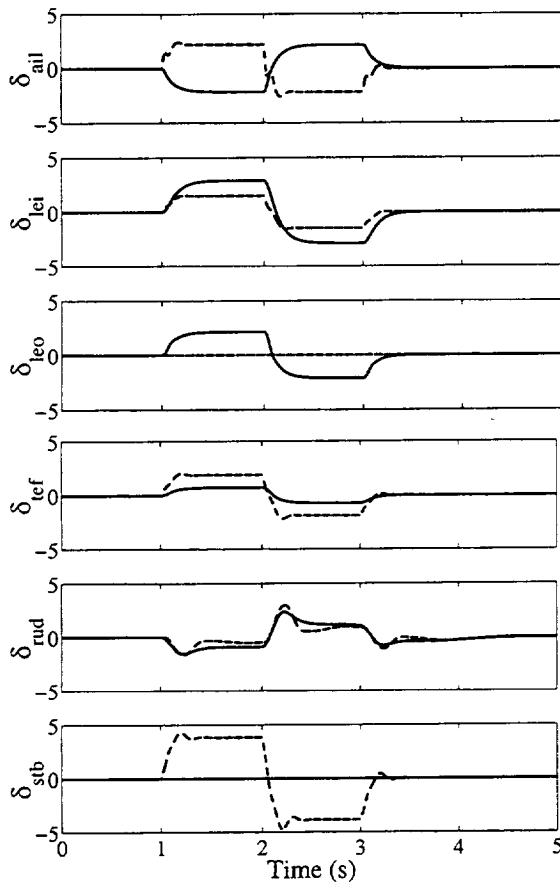

Figure 7: Surface Positions in *deg* during Doublet Maneuver : AAW (—), SRA (— — —)

Figure 7 clearly demonstrates the difference in control allocation for the AAW and SRA aircraft. The stabilator is the main effector for generating roll at this flight condition for the SRA airplane and this surface moves more than any other. Conversely, the stabilator does not move at all during the maneuver for the AAW. The AAW controller accounts for the loss of the powerful stabilator by commanding larger positions for the leading-edge inboard and outboard flaps to generate roll.

The aileron and trailing-edge flaps are noticeably different during the AAW and SRA responses. In particular, the aileron moves in the opposite direction. These differences result from the inclusion of loads minimization as a closed-loop objective. The design model restricted the bending moment to be similar for the AAW and SRA vehicles but allowed the torsion moment to increase for the AAW. The controller for the AAW is positioning these trailing-edge surfaces mainly to achieve the loads objectives because the leading-edge surfaces are already achieving the handling qualities objectives.

The issue of rate saturation for actuators is often more constraining than position saturation so the surface rates during the maneuver are shown in Figure 8. The surface rates are not saturated during the initial stick movement of 1.5 *in*; however, the leading-edge inboard and outboard surfaces are rate saturated for the stick movement of 3 *in*. This saturation is tentatively considered acceptable because it occurs for a very short time, and nonlinear simulations not presented in this paper indicate only a slight lag in the response due to rate limiting.
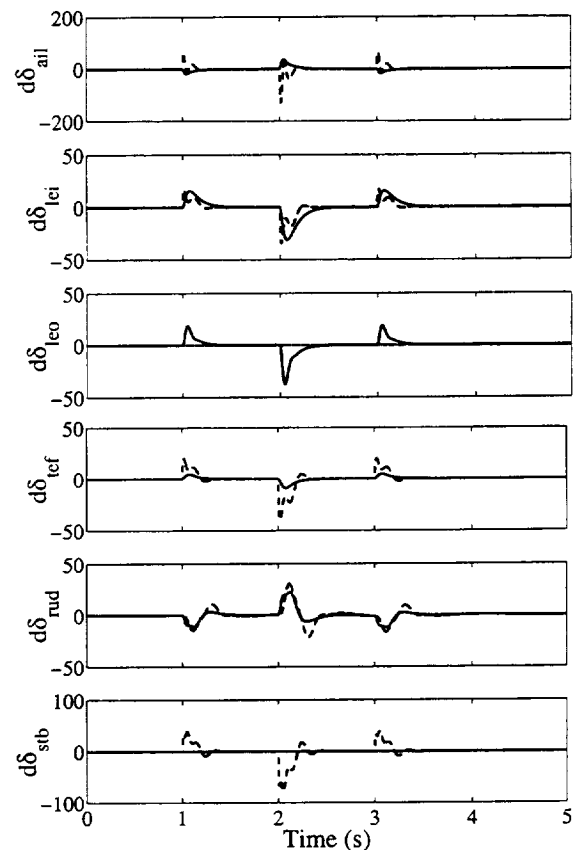
Figure 8: Surface Rates in *deg/s* during Doublet Maneuver : AAW (—), SRA (— — —)

29

The hinge moments on the control surfaces are also of importance for this maneuver because the aircraft is operating at high dynamic pressures. The main concern is for the wing surfaces so the corresponding moments are shown in Figure 9. The hinge moments encountered during the maneuver are generally greater for the AAW than for the SRA but remain within the allowable limits.
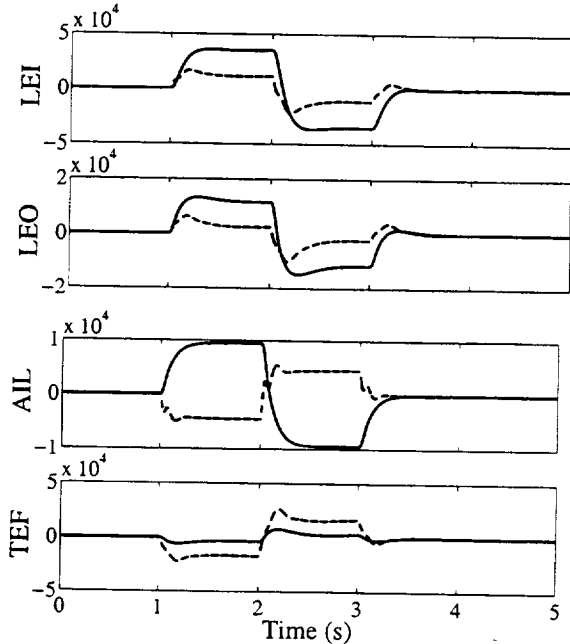

Figure 9: Left-Wing Hinge Moments during Doublet Maneuver : AAW (—), SRA (– – –)

The loads on the structure must be analyzed to demonstrate if the objective of load reduction is achieved and, more importantly, to ensure no loads on the structure exceed the physical limitations. Figure 10 shows that the bending and torsion moment at the wing root is within acceptable levels.
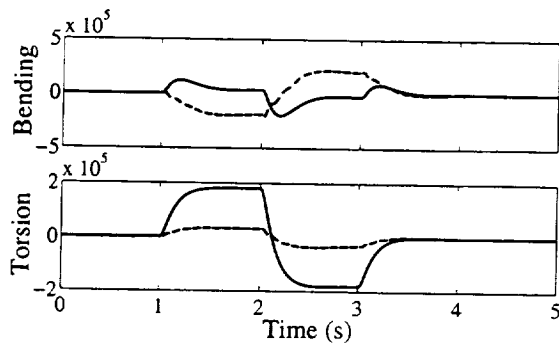

Figure 10: Left-Wing Root Moments during Doublet Maneuver : AAW (—), SRA (– – –)

The load magnitudes in Figure 10 agree with the loads objective that are in the design model. Specifically, the bending moment is similar between the AAW and SRA

but the torsion moment is greater for the AAW than for the SRA. This increase in torsion is expected because the SRA avoids wing twist by using the stabilator to generate roll at this flight condition whereas the AAW commands a wing twist, and consequently torsion, to generate roll. The loads at the wing fold are not shown here but they are similar in nature to the loads at the wing root; namely, the bending moment is smaller for the AAW and the torsion moment is greater but both are within acceptable limits.

5.3. Robustness Analysis

The issue of robustness with respect to modeling uncertainty is an important consideration for predicting the closed-loop properties of the AAW. Some indication of robustness can be obtained by performing extensive Monte Carlo simulations of the full-order nonlinear model; however, a more rigorous evaluation of robustness can be obtained for the linear model by analyzing the structured singular value. This value, μ, reflects whether a model is robust with respect to a set of uncertainty operators [6].

There are several areas of the open-loop model with which uncertainty should be associated. Consider that one of the fundamental flight test objectives of the AAW program is to investigate the technologies associated with modeling of aeroelastic deformation and structural loads at high dynamic pressures. Essentially, full-scale aircraft have not flown with these configurations before so the fidelity of the dynamic models is unclear.

Uncertainty should be associated with the open-loop model to account for potential errors and unmodeled dynamics in the effectiveness of the control surfaces. The model is formulated using static analysis that notes the amount of wing twist that results from placing the control surfaces at any position. This type of model may be overly simplistic because the wing may twist dynamically with nonlinear and time-varying effects.

Introduce a norm-bounded operator, Δ_{in}, to represent a multiplicative uncertainty on the plant input and account for errors in control surface effectiveness. This uncertainty is weighted to allow the error to increase from 5% error near .1 rad/s up to 500% error at high frequencies. This weighting is represented by a diagonal matrix, W_{in}, and associates the same levels of uncertainty with the effectiveness of each control surface.

$$W_{in} = 5\frac{s+5}{s+500}\frac{s+.001}{s+.1}I$$

Uncertainty should also be associated with the output of the open-loop model to account for errors in the amount of roll that is predicted to be generated by wing twist. These predictions are partially based on roll rates that were measured during static testing of partial-scale models in wind tunnels; therefore, errors may occur from is-
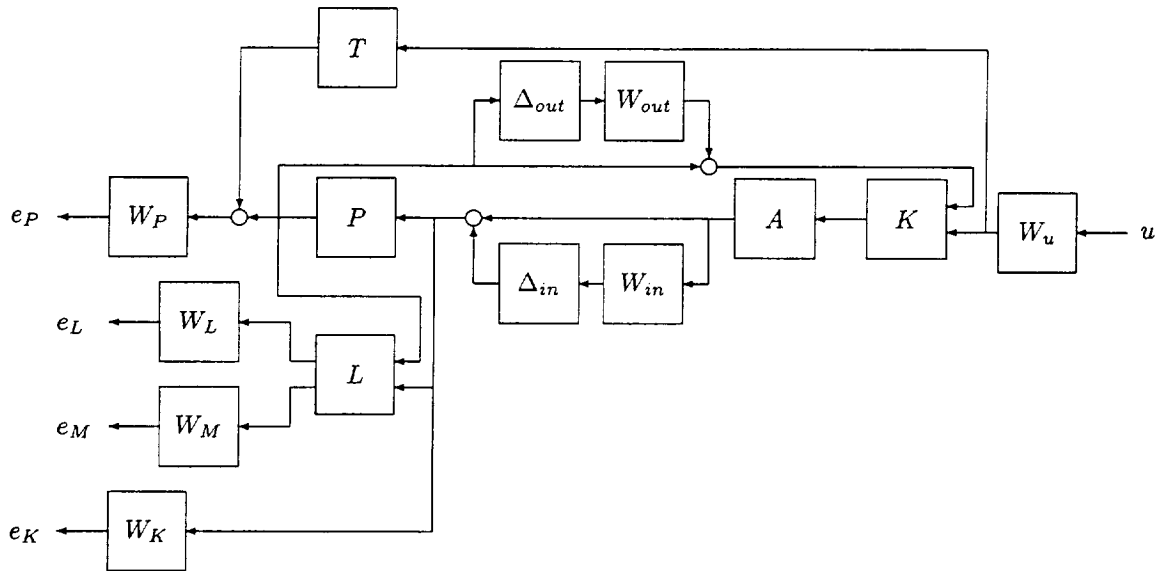
30

Figure 11: Model with Uncertainty Description

sues related to transients, scaling factors, and structural complexities associated with the wing fold.

Associate a norm-bounded operator, Δ_{out}, only with the sensor measurements of the open-loop model that represents errors in roll rate. A weighting function, W_{out}, scales this operator such that the robustness analysis considers errors in roll rate ranging from 10% near .1 *rad/s* to 1000% at high frequencies.

$$W_{out} = 10\frac{s+5}{s+500}\frac{s+.001}{s+.1}$$

Figure 11 presents the closed-loop AAW model with uncertainty operators. Robustness is analyzed by computing μ with respect to Δ_{in} and Δ_{out} for the transfer function from pilot commands to errors.

Figure 12 presents the upper bound for μ that measures robust performance of the closed-loop system. The peak value shows $\mu \leq 1.5$ so the system does not quite meet the desired robustness goal of $\mu < 1$. The peak occurs near the natural frequency associated with the roll mode and agrees with the synthesis that noted the driving constraint for control design was achieving roll performance. Essentially, the controller is optimized to affect this roll mode and consequently is somewhat sensitive to modeling errors.

Also, the robustness of the AAW with the full-order dynamic controller and the approximation used as K_{AAW} is shown in Figure 12. This plot demonstrates that the robustness is quite similar for either closed-loop system. This indicates that the approximation was good and did not severely degrade performance or introduce any sensitivity to modeling errors. Actually, the robustness at lower frequencies is greater for K_{AAW} than for the dy-
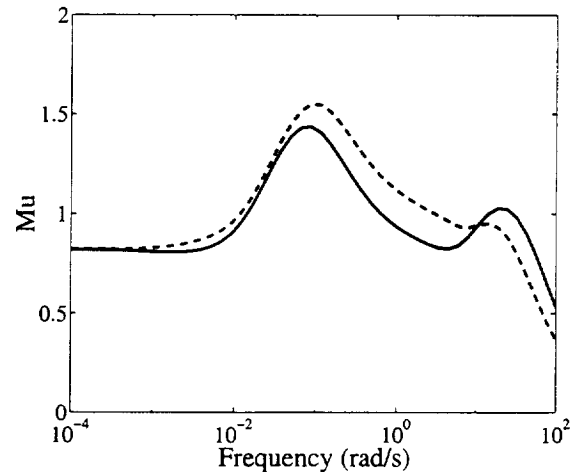

Figure 12: μ for Robust Performance of Error Signals : K_{AAW} (—), Full-Order $\mathcal{H}_\infty$ Controller (— — —)

namic controller so the approximation was able to reduce sensitivity near the roll mode.

6. Control Design as an AAW Technology

The fundamental objective of the AAW program is to demonstrate several areas of technology including aeroservoelastic control; however, the methodology of designing the corresponding controller is generally not considered an AAW technology. This exclusion may be true for certain types of control design but an argument can be made that the $\mathcal{H}_\infty$ approach can greatly facilitate the utilization of AAW technology. Thus, the method of control synthesis may be considered as an indirect, but related, area of AAW technology.

31

The synthesis objective is to minimize the $\mathcal{H}_\infty$ norm of the closed-loop system or equivalently to minimize the maximum size of the errors that result from a pilot command. The nature of the $\mathcal{H}_\infty$ norm directs the synthesis to reduce the size of the largest error and ensure the sizes of all the remaining errors are no greater than this largest error. For example, if the error related to handling qualities or actuator constraints is larger than the error related to loads then the controller does not minimize the loads error.

The $\mathcal{H}_\infty$ approach for control design does not directly perform a loads minimization; rather, the compensator achieves a level of loads control. Essentially, the weighting on the error signal is chosen at a level for which a controller exists that makes the closed-loop $\mathcal{H}_\infty$ norm to be unity. The AAW will achieve the handling qualities and actuator objectives while reducing the loads to less than the values associated with the error weighting if this norm condition is satisfied. In this way, the synthesis performs a simultaneous optimization for loads, handling qualities, actuator, and performance objectives.

This simultaneous optimization suggests that the $\mathcal{H}_\infty$ methodology may be a valuable asset in realizing AAW technology on future aircraft. The ability to simultaneously consider several closed-loop objectives presents a method to easily determine the achievable properties of the aircraft. The designer simply iterates over values of the weighting functions to determine what levels of performance and loads reduction can be achieved for a particular set of actuator constraints. This approach allows a straightforward determination of the benefits that can be achieved by the remaining elements of AAW technology.

7. Concluding Remarks

The Active Aeroelastic Wing program has several objectives that present challenges for control design. This paper presents an $\mathcal{H}_\infty$ approach that encompasses these objectives in the controller synthesis. The design model is formulated by generating errors that relate to handling qualities, performance, actuator, and loads objectives. The resulting controller is designed by simultaneously considering all these closed-loop objectives. A point design is used to demonstrate that the approach generates controllers that achieve these goals.

References

[1]   B.D.O. Anderson and J.B. Moore, *Optimal Control - Linear Quadratic Methods*, Prentice-Hall, Englewood Cliffs, NJ, 1990.

[2]   G. Balas, J. Doyle, K. Glover, A. Packard and R. Smith, *μ-Analysis and Synthesis Toolbox - Users Guide*, The Mathworks, Natick MA, 1991.

[3]   R.L. Bisplinghoff and H. Ashley, *Principles of Aeroelasticity*, Dover Publications, Inc., New York, 1962.

[4]   J. Doyle, K. Glover, P. Khargonekar, and B. Francis, "State-space solutions to standard $\mathcal{H}_2$ and $\mathcal{H}_\infty$ control problems," *IEEE Transactions on Automatic Control*, Vol. 34, No. 8, August 1989, pp. 831-847.

[5]   S.K. Krone, L.D. Arnold, and R.K. Hess, *F/A-18 A/B/C/D Flight Control System Design Report Vol. 1 - System Description and Theory of Operation*, McDonnell Aircraft Company, MDC-A7813, December 1992.

[6]   A. Packard and J. Doyle, "The Complex Structured Singular Value," *Automatica*, Vol. 29, No. 1, 1993, pp. 71-109.

[7]   E. Pendleton, K.E. Griffin, M.W. Kehoe, and B. Perry, "A Flight Research Program for Active Aeroelastic Wing Technology," *AIAA Structures, Structural Dynamics, and Materials Conference*, AIAA-96-1574, April 1996.

[8]   E. Pendleton, D. Bessette, P. Field, G. Miller, and K. Griffin, "The Active Aeroelastic Wing Flight Research Program," *AIAA Structures, Structural Dynamics, and Materials Conference*, AIAA-98-1972, April 1998.

[9]   B. Perry, S.R. Cole, and G.D. Miller, "A Summary of an AFW Program," *Journal of Aircraft*, Vol. 32, No. 1, January 1995.

[10]   J.R. Sitz, *The F-18 Systems Research Aircraft Facility*, NASA-TM-4433, 1992.

[11]   S. Zillmer, *Integrated Structure/Maneuver Design Procedure for Active Aeroelastic Wings - Users Manual*, Wright Laboratory, Dayton OH, WL-97-3037, March 1997.